Available online at www.sciencedirect.com
SCIENCE DIRECT®
Journal of Sound and Vibration 272 (2004) 1–20
JOURNAL OF SOUND AND VIBRATION
www.elsevier.com/locate/jsvi

Vibration suppression of composite sandwich beams

Chyanbin Hwu*, W.C. Chang, H.S. Gai

Institute of Aeronautics and Astronautics, National Cheng Kung University, Tainan 70101, Taiwan, ROC

Received 8 August 2002; accepted 17 March 2003

Abstract

Although some investigations such as buckling and free vibration of composite sandwich beams have been done analytically, very few analytical work about the forced vibration of composite sandwich beams can be found in the literature. In our study, we get the closed-form solution for the free vibration problems and derive an orthogonality relation consisting the effects of rotary inertia and shear deformation. Unlike the usual orthogonality relation for shallow beams in which the modal shapes are the shapes of deflections corresponding to the natural frequencies, the relation for the composite sandwich beams cannot stand without including the rotation angles. Through the establishment of the orthogonality relation, the forced vibration problems can then be solved by modal analysis. The analytical solution of the forced vibration is useful for the study of vibration suppression. In this study we investigate smart composite sandwich beams with surface bonded piezoelectric sensors and actuators. By combining the present vibration analysis with the classical optimal control method, an observed-state feedback control system for the composite sandwich beams is designed. To show the importance of considering the effects of rotary inertia and shear deformation on the natural frequencies and mode shapes of composite sandwich beams, several illustrative examples are done. Numerical examples of vibration suppression of cantilevered composite sandwich beams are also implemented, which show that their first few vibration modes are successfully controlled.

1. Introduction

Because sandwich construction has many advantages over the conventional structural constructions such as high bending stiffness, good weight savings, good surface finish, etc., it has been used in aeronautical applications for more than 50 years. Nowadays, the use of sandwich construction is further enhanced by the introduction of the laminated composites as the faces of sandwich panels. Therefore, it is desirable to have further studies about the composite sandwich

*Corresponding author. Fax: +886-6-238-9940.
E-mail address: chwu@mail.ncku.edu.tw (C. Hwu).

0022-460X/03/$ - see front matter
doi:10.1016/S0022-460X(03)00302-X

structures after knowing their related mechanical behaviors of the composite laminates [1–7]. Fundamental mathematical modelling about the analysis of composite sandwich structures can be found in some published textbooks such as [8–10]. Recently, Noor, et al. [11] collected several published works in their review about the computational models for sandwich panels and shells.

My co-workers and I developed a mathematical model for the buckling and vibration of laminated composite sandwich plates and beams [12–14]. The main difference of our modelling with that of the conventional laminated composite structures is the consideration of transverse shear deformation and rotary inertia. With this modelling, closed-form solutions for the free vibration of composite sandwich beams under various boundary conditions are obtained in this paper, which can also be specialized to their associated problems of composite laminated beams. Moreover, an orthogonality relation consisting the effects of rotary inertia and shear deformation has also been derived. Unlike the usual orthogonality relation for shallow beams in which the modal shapes are the shapes of deflections corresponding to the natural frequencies, the relation for the composite sandwich beams cannot stand without including the rotation angles. Through the orthogonality relation, the mechanical responses of forced vibration can then be found by modal analysis.

Due to the rapid development of intelligent space structure and mechanical systems, advanced structures with integrated self-monitoring and control capabilities are increasingly becoming important. It is also well known that piezoelectric materials produce an electric field when deformed and undergo deformation when subjected to an electric field. Due to this intrinsic coupling phenomenon, piezoelectric materials are widely used as sensors and actuators in intelligent advanced structure design. With this consideration, the sensor and actuator equations were derived based upon our analytical expressions of forced vibration. Employing this result into the classical optimal control algorithm, an observed-state feedback control system is designed and implemented in this paper.

2. Composite sandwich beams

A mathematical model for the mechanical analysis of delaminated composite sandwich plates and beams was proposed by Hwu and Hu [12] for the buckling problems and by Hu and Hwu [13] for the vibration problems. According to their model, the equations of motion for the composite sandwich beams with the effects of rotary inertia and shear deformation included can be expressed as (see Fig. 1)

$$\frac{\partial Q_x}{\partial x} + p = \rho h \frac{\partial^2 w}{\partial t^2}, \qquad \frac{\partial M_x}{\partial x} = Q_x + I \frac{\partial^2 \beta_x}{\partial t^2}, \tag{1a}$$

where

$$Q_x = S\gamma_{xz}, \qquad M_x = D\frac{\partial \beta_x}{\partial x}, \qquad \beta_x = \gamma_{xz} - \frac{\partial w}{\partial x}. \tag{1b}$$

p, Q_x and M_x represent the transverse distributed load, transverse shear stress resultant and bending moment, respectively. w, γ_{xz} and β_x denote the transverse deflection, transverse shear strain and rotation angle. I, ρ and h are, respectively, the moment of inertia (with respect to the

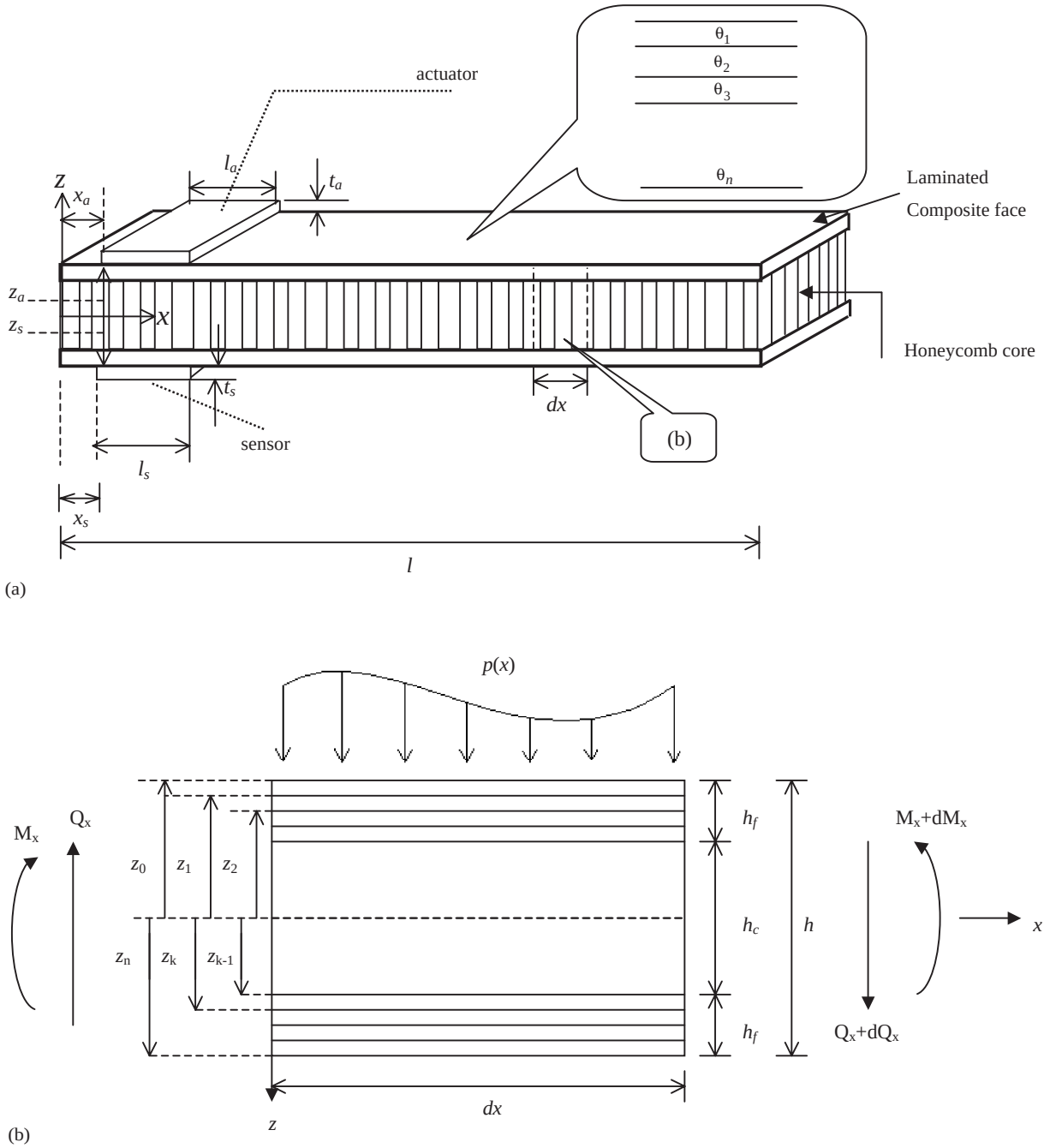

Fig. 1. A composite sandwich beam with piezoelectric sensors and actuators.

midplane), mass density and thickness. S and D are the transverse shear stiffness and bending stiffness whose values can be calculated from the material and section properties of the core and faces of the composite sandwich beams. The mass density ρ for the sandwich may be

approximated by the general mixture rule [15]

$$\rho = (\rho_c h_c + 2\rho_f h_f)/(h_c + 2h_f), \tag{2a}$$

where ρ_c and ρ_f are, respectively, the mass density of core and faces, and h_c and h_f are, respectively, the thickness of core and faces. The moment of inertia I for rectangular cross section with unit width is $I = \rho h^3/12$.

By considering the non-uniform transverse shear stress distribution across the core thickness, the transverse shear stiffness S can be set to [15]

$$S = \alpha h_c G_c, \tag{2b}$$

where G_c is the effective shear modulus of the core; α is the shear coefficient and is selected to be $\alpha = 5/6$ for rectangular cross-section. The bending stiffness D can be calculated from [12]

$$D = D_{11} - \frac{B_{11}^2}{A_{11}}, \tag{2c}$$

where A_{11}, B_{11} and D_{11} are, respectively, the 11 component of the extensional, coupling and bending stiffnesses of the composite sandwiches [15]. Note that the stiffnesses are calculated based upon the midsurface of the sandwich instead of the midsurface of the face laminates [12].

Substituting Eq. (1b) into Eq. (1a) and expressing the equations in terms of the deflection w and the slope β_x, we get

$$S\left(\frac{\partial \beta_x}{\partial x} + \frac{\partial^2 w}{\partial x^2}\right) + p = \rho h \frac{\partial^2 w}{\partial t^2}, \qquad D\frac{\partial^2 \beta_x}{\partial x^2} = S\left(\beta_x + \frac{\partial w}{\partial x}\right) + I\frac{\partial^2 \beta_x}{\partial t^2}. \tag{3}$$

From the first equation of Eq. (3), we can further express $\partial\beta_x/\partial x$ in terms of w. Substituting this expression into the partial differential with respect to x of the second equation of Eq. (3), we obtain the equation of motion in terms of the transverse deflection only, which is

$$D\frac{\partial^4 w}{\partial x^4} - \left(I + \frac{\rho h D}{S}\right)\frac{\partial^4 w}{\partial x^2 \partial t^2} + \frac{\rho h I}{S}\frac{\partial^4 w}{\partial t^4} + \rho h \frac{\partial^2 w}{\partial t^2} = p + \frac{I}{S}\frac{\partial^2 p}{\partial t^2} - \frac{D}{S}\frac{\partial^2 p}{\partial x^2}. \tag{4}$$

After solving the transverse deflection w through the equation of motion (4) and its associated boundary and initial conditions, the slope β_x can be obtained by integrating Eq. $(3)_1$ with respect to x. The transverse shear strain γ_{xz} can then be obtained from the third equation of Eq. (1b).

3. Free vibration

To know the natural frequency and its associated mode of vibration of the composite sandwich beams, we consider the case that the external load $p(x, t) = 0$, i.e., the problems of free vibration. To find the natural modes of vibration, the usual way is the method of separation of variables. By this method we write the deflection $w(x, t)$ as a product of a function $W(x)$ of the spatial variables only and a function $f(t)$ depending on time only. Furthermore, because of free vibration $f(t)$ is harmonic and of frequency ω. Thus,

$$w(x, t) = W(x)\mathrm{e}^{\mathrm{i}\omega t}. \tag{5}$$

Through the use of Eq. (5), the equation of motion (4) can easily be reduced to an ordinary differential equation and the general solutions for $W(x)$ can be obtained as

$$W(x) = c_1 \cosh \lambda x + c_2 \sinh \lambda x + c_3 \cos \mu x + c_4 \sin \mu x, \tag{6a}$$

where

$$\lambda^2 = \frac{\omega^2}{2D}(-\hat{I} + \sqrt{\hat{I}^2 + 4\hat{m}D}), \qquad \mu^2 = \frac{\omega^2}{2D}(\hat{I} + \sqrt{\hat{I}^2 + 4\hat{m}D}) \tag{6b}$$

and

$$\hat{I} = I + \frac{\rho h D}{S}, \qquad \hat{m} = \frac{\rho h}{\omega^2} - \frac{\rho h I}{S}. \tag{6c}$$

The above solutions (6a–c) are valid when $\hat{m} > 0$, or say $\omega^2 < S/I$, which is usually true for the transverse shear deformation neglected since in that case the shear stiffness S is assumed to be infinite. For the case of $\hat{m} < 0$, similar results can be obtained and will not be discussed in this paper. To find the natural frequency and the mode shape, we need to know the boundary conditions of the problems considered. The usual boundary conditions encountered in the vibration of the composite sandwich beams are

$$\text{(i) Simply supported ends}: \; w = M_x = 0 \quad \text{at } x = 0, l, \tag{7a}$$

$$\text{(ii) Clamped}-\text{clamped ends}: \; w = \beta_x = 0 \quad \text{at } x = 0, l, \tag{7b}$$

$$\text{(iii) Clamped}-\text{free ends}: \; w = \beta_x = 0 \quad \text{at } x = 0 \text{ and } Q_x = M_x = 0 \text{ at } x = l. \tag{7c}$$

Substituting the general solution (6a) into the boundary conditions (7a–c), we can obtain the natural frequency and mode shape of the composite sandwich beams. Although these explicit solutions have been shown in our previous work [13] as one of the special cases of the delaminated composite sandwich beams, by careful check we found that there are some errors in our previous solutions. Due to the importance of these solutions to our following discussions, we now like to list these solutions as follows.

(i) Simply supported ends:

$$\mu_j l = j\pi, \tag{8a}$$

$$W_j(x) = \sin(\mu_j x), \quad j = 1, 2, \ldots . \tag{8b}$$

(ii) Clamped–clamped ends:

$$2(1 - \cosh \lambda_j l \cos \mu_j l) + \left(\gamma_j - \frac{1}{\gamma_j}\right) \sinh \lambda_j l \sin \mu_j l = 0, \tag{9a}$$

$$W_j(x) = \cosh \lambda_j x - \cos \mu_j x - \alpha_j(\sinh \lambda_j x - \gamma_j \sin \mu_j x), \quad j = 1, 2, \ldots . \tag{9b}$$

(iii) Clamped–free ends:

$$2 + \left(\frac{\lambda_j}{\mu_j} - \frac{\mu_j}{\lambda_j}\right) \sin \mu_j l \sinh \lambda_j l + \left(\frac{\gamma_j \lambda_j}{\mu_j} + \frac{\mu_j}{\gamma_j \lambda_j}\right) \cos \mu_j l \cosh \lambda_j l = 0, \tag{10a}$$

$$W_j(x) = \cosh \lambda_j x - \cos \mu_j x - \beta_j(\sinh \lambda_j x - \gamma_j \sin \mu_j x), \quad j = 1, 2, \ldots \tag{10b}$$

where

$$\alpha_j = \frac{\cosh \lambda_j l - \cos \mu_j l}{\sinh \lambda_j l - \gamma_j \sin \mu_j l}, \quad \beta_j = \frac{\mu_j \sinh \lambda_j l - \lambda_j \sin \mu_j l}{\mu_j \cosh \lambda_j l + \gamma_j \lambda_j \cos \mu_j l},$$

$$\gamma_j = \frac{\lambda_j + \rho h \omega_j^2 / \lambda_j S}{\mu_j - \rho h \omega_j^2 / \mu_j S}. \tag{10c}$$

In the case of the laminated composite beams that can be considered as a sandwich without core, the thickness of the beam is usually small compared to its length. Therefore, it is reasonable to neglect the effects of rotary inertia and shear deformation for this special but common case. The natural frequency and mode shape of the laminated composite beams can be then obtained by specializing Eqs. ((8)–(10)) with $I = 0$ and $S \to \infty$.

Orthogonality condition: If the family of natural vibration mode shapes $W_j(x)$ can constitute a complete set of orthonormal modes, most of the vibration problems can be solved by modal analysis through the use of the expansion theorem [16]. However, due to the complexity of the partial differential equation (4) which the deflection mode shape should satisfy, it is very difficult to prove that they are orthogonal to each other. Even the direct use of the solutions shown in Eqs. ((8)–(10)) cannot prove that the natural mode $W_j(x)$ only will constitute a complete orthonormal set. This difficulty leads us to think that maybe the orthogonal set contains not only the deflection but also the slope angle due to the inclusion of the effects of rotary inertia and shear deformation. With this consideration we now deal with Eq. (3) instead of Eq. (4). By assuming

$$w(x,t) = W(x)e^{i\omega t}, \quad \beta_x(x,t) = B(x)e^{i\omega t}, \tag{11}$$

and introducing Eq. (11) into Eq. (3) with $p = 0$, we obtain

$$-\rho h \omega^2 W(x) = S(B'(x) + W''(x)), \quad -I\omega^2 B(x) = DB''(x) - SB(x) - SW'(x). \tag{12}$$

Eq. (12) contains two second order homogeneous ordinary differential equations, which must be supplemented by four boundary conditions, i.e., two boundary conditions for each end. Usually, the boundary condition is either displacement-prescribed or forced-prescribed or mixed. For homogeneous boundary conditions, they may be expressed as (i) $w = 0$ or $Q_x = 0$ and (ii) $\beta_x = 0$ or $M_x = 0$. Through the use of relations (1b) and (11), we have

$$\text{(i)} \quad W(x) = 0 \quad \text{or} \quad B(x) + W'(x) = 0, \tag{13a}$$

$$\text{(ii)} \quad B(x) = 0 \quad \text{or} \quad B'(x) = 0. \tag{13b}$$

Different combinations may now provide us four different types of end conditions. They are

$$\text{(i) } \textit{Fixed end}: \quad w = \beta_x = 0 \text{ which leads to } W(x) = B(x) = 0. \tag{14a}$$

$$\text{(ii) } \textit{Free end}: \quad Q_x = M_x = 0 \text{ which leads to } B(x) + W'(x) = B'(x) = 0. \tag{14b}$$

$$\text{(iii) } \textit{Hinged end}: \quad w = M_x = 0 \text{ which leads to } W(x) = B'(x) = 0. \tag{14c}$$

$$\text{(iv) } \textit{Moving end}: \quad Q_x = \beta_x = 0 \text{ which leads to } B(x) + W'(x) = B(x) = 0. \tag{14d}$$

By a simple mathematical manipulation, the natural frequencies and modes of vibration for each different boundary condition can be obtained, which can be proved to be exactly the same as

those shown in Eqs. ((8)–(10)). The natural mode shapes of rotation angles, $B_j(x)$, which are not provided in Eqs. ((8)–(10)) can be obtained by using Eq. $(12)_1$ with the results of $W_j(x)$ obtained in Eqs. ((8)–(10)). They are

(i) *simply supported ends*:

$$B_j(x) = \left(\frac{\rho h\omega_j^2}{\mu_j S} - \mu_j\right)\cos \mu_j x, \tag{15a}$$

(ii) *clamped–clamped ends*:

$$\begin{aligned} B_j(x) = &\left(-\frac{\rho h\omega_j^2}{\lambda_j S} - \lambda_j\right)\sinh \lambda_j x + \left(\frac{\rho h\omega_j^2}{\mu_j S} - \mu_j\right)\sin \mu_j x \\ &+ \left(\frac{\alpha_j \rho h\omega_j^2}{\lambda_j S} + \alpha_j\lambda_j\right)\cosh \lambda_j x + \left(\frac{\alpha_j\gamma_j \rho h\omega_j^2}{\mu_j S} - \alpha_j\gamma_j\mu_j\right)\cos \mu_j x, \end{aligned} \tag{15b}$$

(iii) *clamped–free ends*:

$$\begin{aligned} B_j(x) = &\left(-\frac{\rho h\omega_j^2}{\lambda_j S} - \lambda_j\right)\sinh \lambda_j x + \left(\frac{\rho h\omega_j^2}{\mu_j S} - \mu_j\right)\sin \mu_j x \\ &+ \left(\frac{\beta_j \rho h\omega_j^2}{\lambda_j S} + \beta_j\lambda_j\right)\cosh \lambda_j x + \left(\frac{\beta_j\gamma_j \rho h\omega_j^2}{\mu_j S} - \beta_j\gamma_j\mu_j\right)\cos \mu_j x. \end{aligned} \tag{15c}$$

Let ω_i and ω_j be the two distinct natural frequencies and $W_i(x), B_i(x)$ and $W_j(x), B_j(x)$ be the corresponding natural modes of vibration resulting from the solution of the equations of motion (12) and its associated boundary conditions (13). Consider Eq. (12) corresponding to $\omega_i, W_i(x)$ and $B_i(x)$. If we multiply Eq. $(12)_1$ by $W_j(x)$ and Eq. $(12)_2$ by $B_j(x)$, add them together and integrate both sides of the equation over the beam length L, we obtain

$$\begin{aligned} &-\omega_i^2 \int_0^L (\rho h W_i(x) W_j(x) + I B_i(x) B_j(x))\,\mathrm{d}x \\ &\quad = \int_0^L [S(B_i'(x) + W_i''(x)) W_j(x) + (DB_i'' - SB_i(x) - SW_i'(x)) B_j(x)]\,\mathrm{d}x. \end{aligned} \tag{16}$$

Similarly, another equation can be obtained from Eq. (16) by interchanging the subscripts i and j. Subtracting these two equations, we get

$$\begin{aligned} &(\omega_i^2 - \omega_j^2)\int_0^L (\rho h W_i(x) W_j(x) + I B_i(x) B_j(x))\,\mathrm{d}x \\ &\quad = \int_0^L S[B_j'(x) W_i(x) + W_j''(x) W_i(x) - B_i'(x) W_j(x) - W_i''(x) W_j(x)] \\ &\qquad + [(DB_j''(x) - SB_j(x) - SW_j'(x)) B_i(x) - (DB_i''(x) - SB_i(x) - SW_i'(x)) B_j(x)]\,\mathrm{d}x. \end{aligned} \tag{17}$$

By means of integration by parts, for example,

$$\int_0^L B_j'(x)W_i(x)\,\mathrm{d}x = W_i(x)B_j(x)\Big|_0^L - \int_0^L B_j(x)W_i'(x)\,\mathrm{d}x, \tag{18}$$

the right-hand side of Eq. (17) can be rewritten as

$$\begin{aligned}&\{S[W_i(x)(B_j(x)+W_j'(x)) - W_j(x)(B_i(x)+W_i'(x))]\\ &\quad + D[B_i(x)B_j'(x) - B_j(x)B_i'(x)]\}|_0^L.\end{aligned} \tag{19}$$

The substitution of the end conditions (13) now makes Eq. (19) equivalent to zero. Thus, Eq. (17) reduces to

$$(\omega_i^2 - \omega_j^2)\int_0^L (\rho h W_i(x)W_j(x) + IB_i(x)B_j(x))\,\mathrm{d}x = 0 \tag{20}$$

or

$$\begin{aligned}\textstyle\int_0^L(\rho h W_i(x)W_j(x) + IB_i(x)B_j(x))\,\mathrm{d}x = 0, &\quad \text{when } \omega_i \neq \omega_j,\\ \neq 0, &\quad \text{when } \omega_i = \omega_j.\end{aligned} \tag{21}$$

Through normalization, (21) can be combined into

$$\int_0^L (\rho h W_i(x)W_j(x) + IB_i(x)B_j(x))\,\mathrm{d}x = \delta_{ij}, \tag{22}$$

where δ_{ij} is the Kronecker delta. Unlike the usual orthogonality conditions for the cases that the effects of rotary inertia and shear deformation are neglected, the orthogonality found in Eq. (22) shows that the complete set includes not only the mode shapes of the deflection but also the slope angle.

4. Forced vibration

To study the forced vibration problem, one usually starts from the equation of motion. In this paper, two equivalent expressions are provided. One is two equations of Eq. (3) which is based on two basic functions w and β_x, and the other is a single equation of Eq. (4) which is based on w. Without deliberative consideration, most of the studies may choose the single equation (4) as the basic equation of motion. However, due to the appearance of the transverse shear stiffness S and the moment of inertia I, it is not easy to apply the usual approach of modal analysis to decouple the equation of motion into a set of uncoupled differential equations. From the discussion of the previous section, we see that the orthogonality condition (22) contains not only the mode shapes of the transverse deflection but also the mode shapes of the slope. This orthogonality condition gives us a great hint that the forced vibration analysis should start from the two-equations of Eq. (3) instead of the single equation of Eq. (4). With this understanding, we may now employ the expansion theorem to obtain the system response by modal analysis. Using the expansion theorem we write the solution of Eq. (3) as a superposition of the natural modes $W_j(x)$ and $B_j(x)$

multiplying corresponding time-dependent generalized coordinates $\eta_j(t)$. Hence,

$$w(x,t)=\sum_{j=1}^{\infty} W_j(x)\eta_j(t), \quad \beta_x(x,t)=\sum_{j=1}^{\infty} B_j(x)\eta_j(t) \tag{23}$$

and introducing Eq. (23) into Eq. (3), we obtain

$$\rho h\sum_{j=1}^{\infty} W_j(x)\ddot{\eta}_j(t)=\sum_{j=1}^{\infty} S(B_j'(x)+W_j''(x))\eta_j(t)+p(x,t),$$

$$I\sum_{j=1}^{\infty} B_j(x)\ddot{\eta}_j(t)=\sum_{j=1}^{\infty} (DB_j'(x)-SB_j(x)-SW_j'(x))\eta_j(t). \tag{24}$$

Employing the results of Eq. (12) in Eq. (24), we get

$$\rho h\sum_{j=1}^{\infty} W_j(x)\ddot{\eta}_j(t)=-\sum_{j=1}^{\infty} \rho h\omega_j^2 W_j(x)\eta_j(t)+p(x,t),$$

$$I\sum_{j=1}^{\infty} B_j(x)\ddot{\eta}_j(t)=-\sum_{j=1}^{\infty} I\omega_j^2 B_j(x)\eta_j(t). \tag{25}$$

Multiplying Eq. $(25)_1$ by $W_i(x)$ and Eq. $(25)_2$ by $B_i(x)$, adding them together and integrating both sides of the equation over the beam length L, we obtain

$$\left\{\sum_{j=1}^{\infty}(\ddot{\eta}_j(t)+\omega_j^2\eta_j(t))\int_0^L (\rho h W_j(x)W_i(x)+IB_j(x)B_i(x))\,\mathrm{d}x\right\}$$

$$=\int_0^L p(x,t)W_i(x)\,\mathrm{d}x. \tag{26}$$

Through the use of the orthogonality condition found in Eq. (22), an infinite set of *uncoupled* second order ordinary differential equation system is obtained as

$$\ddot{\eta}_j(t)+\omega_j^2\eta_j(t)=N_j(t), \quad j=1,2,\ldots, \tag{27a}$$

where $N_j(t)$ denotes a generalized force associated with the generalized coordinate $\eta_j(t)$ and is related to the transverse distributed load q by

$$N_j(t)=\int_0^L p(x,t)W_j(x)\,\mathrm{d}x. \tag{27b}$$

5. Piezoelectric sensors and actuators

To suppress the vibration of the composite sandwich beams, we consider the popular way by bonding piezoelectric sensors and actuators on the surfaces of the beam. It is well known that piezoelectric materials produce an electric field when deformed and undergo deformation when subjected to an electric field. Due to this intrinsic coupling phenomenon, piezoelectric materials are widely used as the sensors and actuators in intelligent advanced structure design. The

piezoelectric sensors can respond to structural vibration and generate output voltage due to the direct piezoelectric effect. On the other hand, the actuators can induce force and moment and control the system due to the converse piezoelectric effect. The piezoelectric properties can be described as a constitutive relation which characterizes the coupling effects between mechanical and electrical properties as follows:

$$D_i = e_{ik}\varepsilon_k + \varepsilon_{ij}^S E_j, \quad \varepsilon_k = S_{il}^E \sigma_l + d_{jk} E_j, \quad i,j = 1,2,3, \quad k,l = 1,2,\ldots,6, \tag{28}$$

where σ_l and ε_k represent the stress and strain, respectively; D_i and E_j represent the electric displacement and electric field, respectively. e_{ik}, ε_{ij}^S, S_{il}^E and d_{jk} represent the piezoelectric stress constant, electric permittivity, elastic compliance and piezoelectric strain coefficient, respectively.

Note that in the following derivation of sensor and actuator equations, the assumption of the perfect bond between the piezoelectric sensors/actuators and the composite sandwich beams has been made. Therefore, the validity of our results will depend on this assumption. In real applications, this assumption may be influenced by the flexibility/rigidity of sensors and actuators. Hence, if a piezo-ceramics is selected to be an actuator, due to its significant large rigidity, the length of the actuator should be small enough to conform to the perfect bond assumption.

Sensor equation: If the composite sandwich beams deform under a certain external load, the axial strain ε_1 on the surface of piezoelectric sensor which was attached on the beam will be $\varepsilon_1 = z_s \partial\beta_x/\partial x$ where z_s is the distance from the piezoelectric sensor to the mid-surface. By Eq. $(28)_1$, we know this strain will induce an electric displacement D_3 in the thickness direction as $D_3 = e_{31}\varepsilon_1$. The electric charge of the sensor region Ω_s corresponding to this electric displacement is $q_s = \int_{\Omega_s} D_3 \, \mathrm{d}x$. By using Eq. $(23)_2$ for the expansion of the rotation angle, the sensor charge can finally be expressed as a linear combination of the generalized co-ordinates η_j, which is

$$q_s = \sum_{j=1}^{\infty} c_j \eta_j(t), \quad c_j = z_s e_{31} \int_{\Omega_s} B_j'(x) \, \mathrm{d}x. \tag{29}$$

In the case of several sensors attached on the beam, the electric charge $q_s^{(i)}$ over each sensor region $\Omega_s^{(i)}$ can be expressed as

$$q_s^{(i)} = \sum_{j=1}^{\infty} c_j^{(i)} \eta_j(t), \quad c_j^{(i)} = z_s e_{31} \int_{\Omega_s^{(i)}} B_j'(x) \, \mathrm{d}x, \quad i = 1,\ldots,n_s, \tag{30}$$

where n_s is the number of the sensors.

Actuator equation: To suppress the vibration, a control force is actuated through the piezoelectric actuators. By applying a voltage V_a in the thickness direction, an electric field E_3 ($= V_a/t_a$, where t_a is the thickness of the piezoelectric actuators) is generated, which will induce an axial strain $\varepsilon_1^a = d_{31}E_3$ on the piezoelectric actuators. Due to the assumption of the perfect bonding, the axial strain of the composite sandwich beams caused by the deformation of the piezoelectric actuator may be written as $\varepsilon_1 = z\varepsilon_1^a/z_a$, where z_a is the distance from the piezoelectric actuator to the mid-surface and z is the co-ordinate in the thickness direction. Note that the linear variation of ε_1 with respect to z is the basic assumption of the formulation provided

in Eq. (1). The bending moment M_x^a induced by the actuator can therefore be calculated by

$$M_x^a = \sum_{k=1}^{n} \int_{h_{k-1}}^{h_k} \sigma_1^{(k)} z \, \mathrm{d}z = \sum_{k=1}^{n} \int_{h_{k-1}}^{h_k} (\bar{Q}_{11}^{(k)} \varepsilon_1) z \, \mathrm{d}z$$
$$= \sum_{k=1}^{n} \int_{h_{k-1}}^{h_k} \bar{Q}_{11}^{(k)} \left(\frac{z}{z_a} \varepsilon_1^a \right) z \, \mathrm{d}z = k_a V_a, \tag{31a}$$

where

$$k_a = \frac{D_{11} d_{31}}{z_a t_a}. \tag{31b}$$

The equivalent transverse distributed load p_a can then be obtained by using the relation $p = -\partial^2 M_x / \partial x^2$, i.e.,

$$P_a = -\partial^2 (k_a V_a) / \partial x^2. \tag{32}$$

By substituting Eq. (32) into Eq. (27b), the generalized force $N_j(t)$ induced by the applied voltage $V_a(t)$ can be found to be

$$N_j(t) = b_j V_a(t), \quad b_j = \int_{\Omega_a} k_a \frac{\partial^2 W_j(x)}{\partial x^2} \, \mathrm{d}x, \tag{33}$$

where Ω_a is the actuator region that the voltage $V_a(t)$ applies. In the case of several actuators attached on the beam, the generalized force $N_j(t)$ induced by all the applied voltage $V_a^{(i)}(t)$ over the region $\Omega_a^{(i)}$, $i = 1, 2, \ldots, n_a$, is

$$N_j(t) = \sum_{i=1}^{n_a} b_j^{(i)} V_a^{(i)}(t), \quad b_j^{(i)} = \int_{\Omega_a^{(i)}} k_a \frac{\partial^2 W_j(x)}{\partial x^2} \, \mathrm{d}x. \tag{34}$$

As we mention at the beginning of this section, the validity of the sensor and actuator equations will depend on the assumption of the perfect bond between the sensors/actuators and the composite sandwich beams. Therefore, if the sensors and/or the actuators are rigid, the regions $\Omega_s^{(i)}$ and $\Omega_a^{(i)}$ used in Eqs. (30) and (34) should be small relative to the beam length.

6. Vibration suppression

In control, it is customary to work with state equations instead of configuration equations (27). By applying the generalized force given in Eq. (34) and the sensor charge obtained in Eq. (30), and considering the process and measurement noise $\mathbf{v}(t)$ and $\mathbf{s}(t)$, the state space equation corresponding to Eqs. (27), (30) and (34) for the composite sandwich beams can be written as

$$\dot{\mathbf{x}}(t) = \mathbf{A}\mathbf{x}(t) + \mathbf{B}\mathbf{u}(t) + \mathbf{v}(t),$$
$$\mathbf{y}(t) = \mathbf{C}\mathbf{x}(t) + \mathbf{s}(t), \tag{35a}$$

where

$$\mathbf{x}(t)=\begin{Bmatrix}\mathbf{x}_1(t)\\ \mathbf{x}_2(t)\\ \mathbf{x}_3(t)\\ \vdots\end{Bmatrix},\qquad \mathbf{u}(t)=\begin{Bmatrix}V_a^{(1)}\\ V_a^{(2)}\\ \vdots\\ V_a^{(n_a)}\end{Bmatrix},\qquad \mathbf{y}(t)=\begin{Bmatrix}q_s^{(1)}\\ q_s^{(2)}\\ \vdots\\ q_s^{(n_s)}\end{Bmatrix}, \tag{35b}$$

$$\mathbf{A}=\operatorname{diag}(\mathbf{A}_j),\qquad \mathbf{B}=\begin{Bmatrix}\mathbf{B}_1\\ \mathbf{B}_2\\ \mathbf{B}_3\\ \vdots\end{Bmatrix},\qquad \mathbf{C}=[\mathbf{C}_1\quad \mathbf{C}_2\quad \mathbf{C}_3\quad \cdots] \tag{35c}$$

and

$$\mathbf{x}_j(t)=\begin{Bmatrix}\eta_j(t)\\ \dot{\eta}_j(t)\end{Bmatrix},\quad \mathbf{A}_j=\begin{bmatrix}0 & 1\\ -\omega_j^2 & 0\end{bmatrix},\quad \mathbf{B}_j=\begin{bmatrix}0 & 0 & \cdots & 0\\ b_j^{(1)} & b_j^{(2)} & \cdots & b_j^{(n_a)}\end{bmatrix},$$

$$\mathbf{C}_j=\begin{bmatrix}c_j^{(1)} & 0\\ c_j^{(2)} & 0\\ \vdots & \vdots\\ c_j^{(n_s)} & 0\end{bmatrix}. \tag{35d}$$

The problem now becomes how to apply the control voltage $\mathbf{u}(t)$ to suppress the vibration and how to estimate the full state vector $\mathbf{x}(t)$ by measuring the sensor output $\mathbf{y}(t)$. An effective approach to the control of structures is feedback control. In general, the non-linear distributed control is not feasible, so that a linear control is usually considered. That is, the control force is linear proportional to the deflection and/or its velocity. In this paper, we consider

$$\mathbf{u}(t)=-\mathbf{G}\hat{\mathbf{x}}(t), \tag{36}$$

where $\hat{\mathbf{x}}(t)$ is an estimated state which is introduced to estimate the full state vector $\mathbf{x}(t)$ from the sensor output $\mathbf{y}(t)$; $\mathbf{G}$ is the control gain which should be determined such that the motion of the structure approaches zero asymptotically.

A state estimator also known as an observer for Eq. (35) is assumed to have the form

$$\dot{\hat{\mathbf{x}}}(t)=\mathbf{A}\hat{\mathbf{x}}(t)+\mathbf{B}\mathbf{u}(t)+\hat{\mathbf{K}}(\mathbf{y}(t)-\mathbf{C}\hat{\mathbf{x}}(t)), \tag{37}$$

where $\hat{\mathbf{K}}$ is the Kalman filter gain matrix and can be determined by minimizing the expected value, $E\{(\mathbf{x}-\hat{\mathbf{x}})^{\mathrm{T}}(\mathbf{x}-\hat{\mathbf{x}})\}$. For steady state case, the optimal observer gain matrix $\hat{\mathbf{K}}$ has been found to be [16]

$$\hat{\mathbf{K}}=\mathbf{P}\mathbf{C}^{\mathrm{T}}\mathbf{S}^{-1}, \tag{38a}$$

where the matrix $\mathbf{P}$ satisfying the Riccati equation

$$\mathbf{A}\mathbf{P}+\mathbf{P}\mathbf{A}^{\mathrm{T}}+\mathbf{V}-\mathbf{P}\mathbf{C}^{\mathrm{T}}\mathbf{S}^{-1}\mathbf{C}\mathbf{P}=\mathbf{0}. \tag{38b}$$

$\mathbf{V}(t)$ and $\mathbf{S}(t)$ are the intensities of assumed white noise $\mathbf{v}(t)$ and $\mathbf{s}(t)$ so that the correlation matrices have the forms $E\{\mathbf{v}(t_1)\mathbf{v}^{\mathrm{T}}(t_2)\} = \mathbf{V}(t_1)\delta(t_2 - t_1)$ and $E\{\mathbf{s}(t_1)\mathbf{s}^{\mathrm{T}}(t_2)\} = \mathbf{S}(t_1)\delta(t_2 - t_1)$, respectively.

The optimal control gain $\mathbf{G}$ is then determined by minimizing the performance measure $J = \int_0^{t_f}(\mathbf{x}^{\mathrm{T}}\mathbf{Q}\mathbf{x} + \mathbf{u}^{\mathrm{T}}\mathbf{R}\mathbf{u})\,\mathrm{d}t$ in which t_f is the final time, $\mathbf{Q}$ and $\mathbf{R}$ are, respectively, the state weight matrix and control weight matrix. For a more rapid vibration reduction a larger value of $\mathbf{Q}$ can be selected, while for a smaller energy consumption a larger value of $\mathbf{R}$ can be selected. With an appropriate selection of the weight matrices, the optimal control gain can be found as [16]

$$\mathbf{G} = \mathbf{R}^{-1}\mathbf{B}^{\mathrm{T}}\mathbf{K}, \tag{39a}$$

where $\mathbf{K}$ satisfies the steady state matrix Riccati equation, i.e.,

$$\mathbf{A}^{\mathrm{T}}\mathbf{K} + \mathbf{K}\mathbf{A} + \mathbf{Q} - \mathbf{K}\mathbf{B}\mathbf{R}^{-1}\mathbf{B}^{\mathrm{T}}\mathbf{K} = \mathbf{0}. \tag{39b}$$

Substituting Eq. (36) into Eq. (37) with the control gain $\mathbf{G}$ given in Eq. (39), the estimated state $\hat{\mathbf{x}}(t)$ can be computed by solving the ordinary differential equations (37). The control voltage $\mathbf{u}(t)$ calculated by Eq. (36) is then applied to suppress the vibration. The actual state $\mathbf{x}(t)$ can therefore be calculated from Eq. $(35a)_1$.

The characteristics of the control system can also be described in the following way. First, we obtain the observer error equation by subtracting Eq. (37) from Eq. $(35a)_1$. Then, with $\mathbf{u}(t)$ given in Eq. (36) we rewrite Eq. $(35a)_1$ in terms of the actual state $\mathbf{x}(t)$ and the error $\mathbf{e}(t) = \mathbf{x}(t) - \hat{\mathbf{x}}(t)$. By combining these two equations, the dynamics of the observed-state feedback control system can now be described as

$$\begin{Bmatrix} \dot{\mathbf{x}}(t) \\ \dot{\mathbf{e}}(t) \end{Bmatrix} = \begin{bmatrix} \mathbf{A} - \mathbf{B}\mathbf{G} & \mathbf{B}\mathbf{G} \\ 0 & \mathbf{A} - \hat{\mathbf{K}}\mathbf{C} \end{bmatrix} \begin{Bmatrix} \mathbf{x}(t) \\ \mathbf{e}(t) \end{Bmatrix} + \begin{Bmatrix} \mathbf{v}(t) \\ \mathbf{v}(t) - \hat{\mathbf{K}}\mathbf{s}(t) \end{Bmatrix}. \tag{40}$$

By solving the ordinary differential equation system (40), the dynamic response $\mathbf{x}(t)$ of the control system can easily be calculated. The associated transverse deflection w and rotation angle β_x can then be obtained from Eq. (23).

The control procedure discussed in this section is called an LQG/LTR (linear quadratic Gaussian with loop transfer recovery) control method which uses a Kalman filter as an observer and a controller that minimizes an objective function of quadratic form [17]. A block diagram of the closed-loop LQG/LTR system with a state estimator is shown in Fig. 2.

7. Numerical examples and discussions

In order to design an LQG/LTR controller, the natural frequencies and mode shapes provided by Eqs. (8)–(10) and (15) should be verified. Several examples have been done and compared with the existing results published in the literature [18]. The comparison shows that our solutions presented in Eqs. (8)–(10) and (15) are correct. To save the space of this paper, only one example concerning the free vibration of cantilevered isotropic sandwich beam is shown below. The material properties, dimensions, and cross-sectional data for the isotropic sandwich beams are

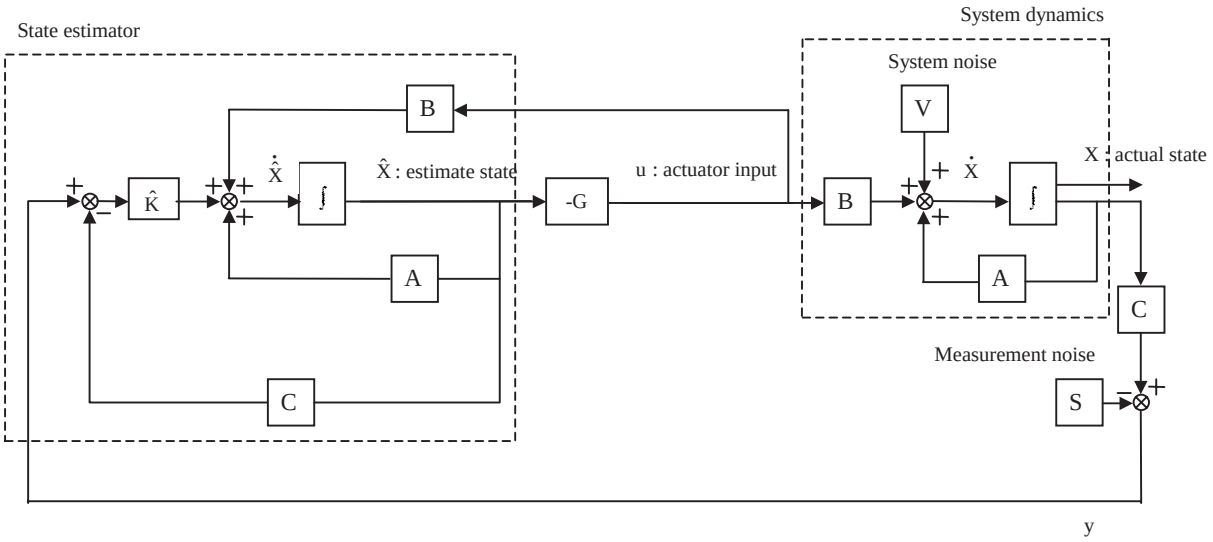

Fig. 2. A block diagram of closed-loop LQG/LTR system with a state estimator.

Table 1
Comparison of natural frequencies

Mode	Ahmed [19]	Mead [20]	Present
Simply supported end			
1	55	56	54
2	—	—	212
3	451	459	457
4	—	—	770
5	1073	1107	1130
Clamped–free end			
1	32	34	32
2	193	202	193
3	499	523	509
4	888	823	923
5	1320	1974	1402

taken from Ref. [19], which are

$$E_f = 68.9 \text{ GPa}, \ h_f = 0.4572 \text{ mm}, \ \rho_f = 2680 \text{ kg/m}^3,$$
$$G_c = 0.08274 \text{ GPa}, \ h_c = 12.7 \text{ mm}, \ \rho_c = 32.8 \text{ kg/m}^3,$$
$$l = 0.7112 \text{ m}.$$

The comparison of the natural frequencies of our results with those presented in the literature is shown in Table 1. The results show that they are well agreed each other even they are obtained from different methods. The merits of our present solutions are that they are analytical

closed-form solutions which could save us a lot of time in computing the natural frequencies and vibration modes, and could help us to know the vibration problems more directly from the mathematical formulae. However, our solutions are not suitable for complicated geometric problems in which the finite element method shows its power [18].

To show the performance of the LQG/LTR controller designed in this paper for the vibration suppression of composite sandwich beams, a cantilevered composite sandwich of the type $[0/0/90/90/0/0/core]_s$ is considered. The material properties, dimensions, and cross-sectional data for the composite sandwich beams are

$$E_L = 130 \text{ GPa}, \quad E_T = 10 \text{ GPa}, \quad v_{LT} = 0.25, \quad G_{LT} = 4.85 \text{ GPa},$$
$$\rho_f = 1480 \text{ kg/m}^3, \quad h_f = 0.2286 \text{ mm},$$
$$G_c = 0.08274 \text{ GPa}, \quad \rho_c = 32.8 \text{ kg/m}^3, \quad h_c = 12.7 \text{ mm},$$
$$l = 0.7112 \text{ m}.$$

Although our analysis presented in Section 5 can be applied to multiple sensors and actuators, for simplicity of illustration only one sensor and actuator are selected in the following example. The material used for the sensor is piezo-film (PFS LDT2-028K) and that for the actuator is piezo-ceramics (Fuji C82). The material properties, locations, and dimensions of the piezoelectric sensor and actuator are [6]

$$\text{sensor}: \quad e_{31} = 6.47 \times 10^{-2} \text{ C/m}^2, \ x_s = 20 \text{ mm}, \ z_s = -6.5786 \text{ mm}, \ l_s = 20 \text{ mm}, \ t_s = 0.028 \text{ mm},$$
$$\text{actuator}: \quad d_{31} = -260 \text{ pC/N}, \ x_a = 20 \text{ mm}, \ z_a = 6.5786 \text{ mm}, \ l_a = 20 \text{ mm}, \ t_a = 0.4 \text{ mm}.$$

The maximum output voltage was limited to 3000 V. The state weight matrix $\mathbf{Q}$ and the control weight matrix $\mathbf{R}$ were selected as $\mathbf{Q} = Q_a\mathbf{I}, \mathbf{R} = R_a\mathbf{I}$, where $\mathbf{I}$ is the unit matrix and the value of Q_a and R_a were determined by trial-and-error method to most effectively control the beam within the desired parameters. In our examples, $Q_a/R_a = 6 \times 10^9$.

Fig. 3 shows the simulation results of open-loop response and LQG/LTR-controlled response for initial conditions corresponding to the first mode vibration. By adding the possible noise from process and measurement, their associated simulation results are shown in Fig. 4 with the intensities of assumed white noise $\mathbf{V}(t)$ and $\mathbf{S}(t)$ selected to be

$$\mathbf{V}(t) = v\begin{bmatrix} 0 & 0 \\ 0 & 1 \end{bmatrix}, \quad \mathbf{S}(t) = s, \quad \text{where } v = 10^{-3} \text{ 1/s}^2, \quad s = 10^{-7} \text{ C/m}.$$

The simulation results are obtained from the analytical model developed in this paper with the aid of MATLAB/Simulink. As can be seen from Figs. 3 and 4, LQG/LTR controller successfully suppresses the vibration of the composite sandwich beam within 1.5 s.

In Figs. 3 and 4, the LQG/LTR controller is designed based upon the first mode of the composite sandwich beams because the disturbance to be controlled is excited by the first mode vibration. However, in the system of composite sandwich beams, there are infinite vibration modes. If our controller is designed only based upon the first mode, it is then possible to lead a result that the vibration cannot be suppressed effectively if the initial vibration includes not only

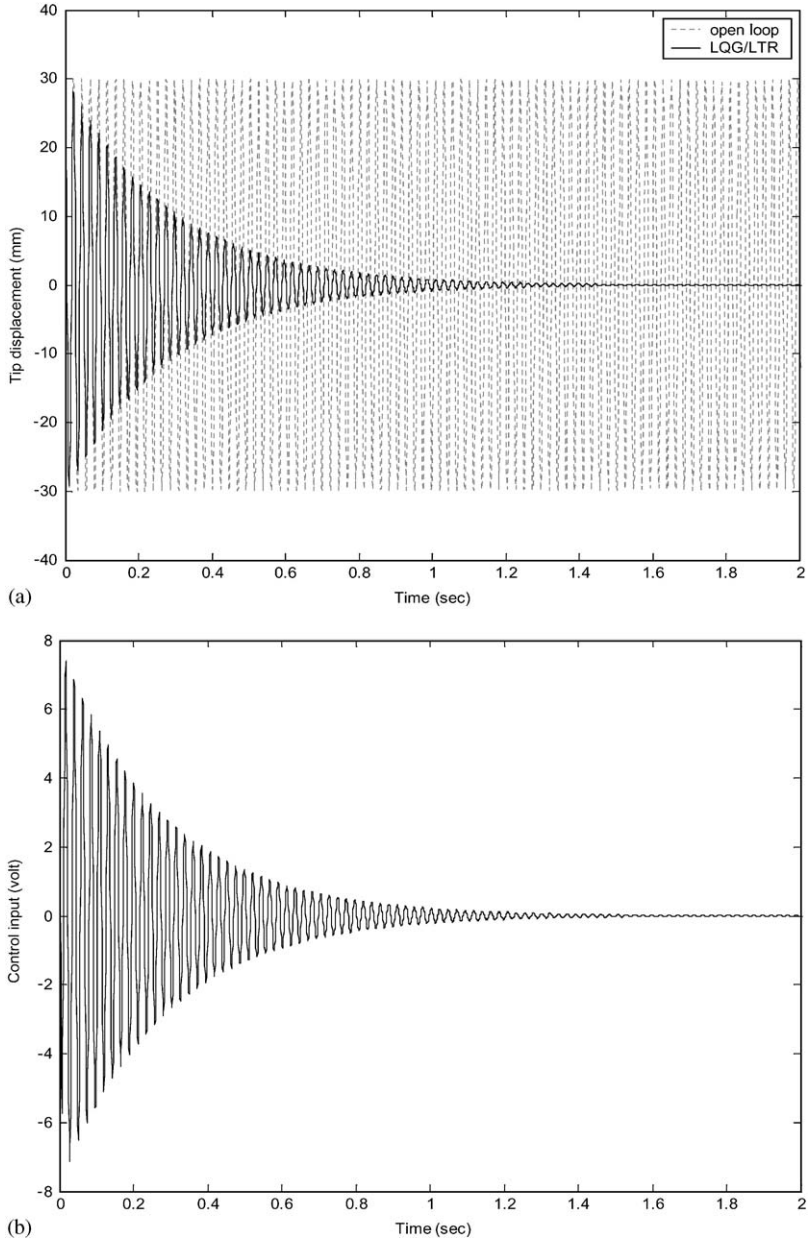

Fig. 3. Vibration suppression of the composite sandwich beam with first mode initial condition: (a) tip–displacement response, (b) control input.

the first mode deflection. To improve this possible ill-controlled problem, one may design a controller based upon several vibration modes. To illustrate the performance of this kind of controller, an example based upon the first five modes is designed and its corresponding result for the mixed mode initial condition is shown in Fig. 5. Here, the initial condition is given by equal

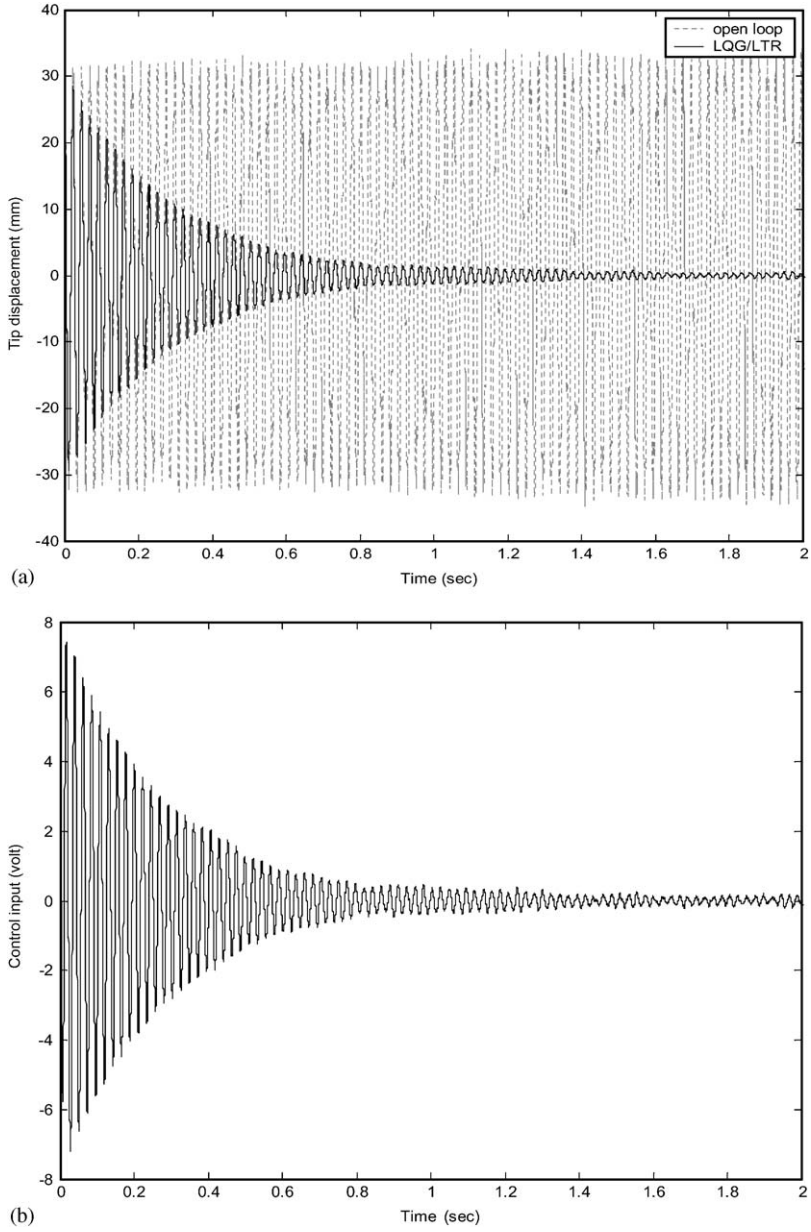

Fig. 4. Consideration of process and measurement noise: (a) tip–displacement response, (b) control input.

distribution among the first five modes. The result of Fig. 5 shows that mode 1 LQG/LTR controller cannot suppress the vibration while first five modes LQG/LTR controller successfully suppresses the vibration within 1.5 s. To monitor the vibration reduction effects, we use an fast Fourier transform (FFT) analyzer through which the tip displacement frequency response of the sandwich beam is plotted in Fig. 6. This figure shows that the LQG/LTR control does not change the first five natural frequencies but reduces the peak values of the first five modes.

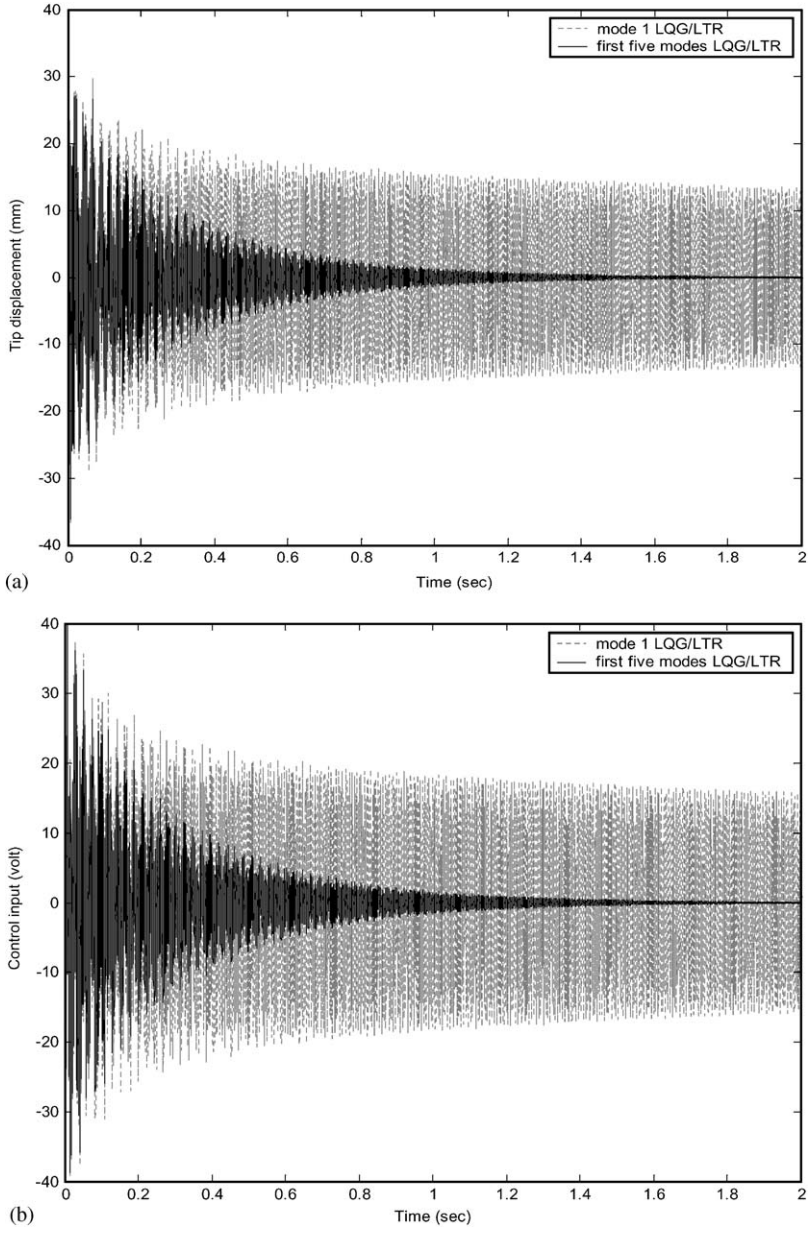

Fig. 5. Vibration suppression of the composite sandwich beam with mixed mode initial condition: (a) tip–displacement response, (b) control input.

8. Conclusions

Analytical solutions for the free and forced vibration of composite sandwich beams are obtained in this paper. In our solutions, the effects of transverse shear deformation and rotary inertia are considered because the sandwich beams are usually relatively thicker. Based upon the

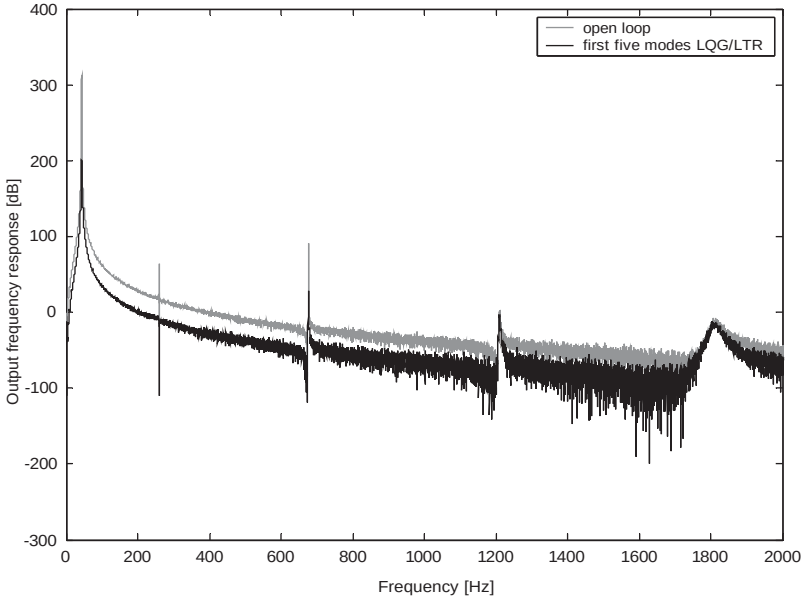

Fig. 6. Frequency response plot of controlled composite sandwich beams.

analytical results for the forced vibration, the sensor equation and actuator equation associated with the surface bonded piezoelectric sensors and actuators are also derived. An LQG/LTR controller is then designed on the basis of these analytical solutions, in which the Kalman filter has been used as an observer and the control gain has been determined to minimize a linear quadratic performance index. The correctness of the natural frequencies and mode shapes provided by our analytical solutions is verified by comparing with the existing numerical solutions. The performance of LQG/LTR controller is then studied under various aspects such as consideration of process and measurement noise, different initial vibration, and design based upon several modes. All these results show that the simulation obtained from the analytical model developed in this paper can successfully suppress the vibration of composite sandwich beams.

Acknowledgements

The authors would like to thank the National Science Council, Republic of China, for support through Grant NSC 90-2212-E-006-173. They also like to thank Mr M.C. Yu for plotting some of the figures.

References

[1] E.F. Crawley, J.D. Luis, Use of piezoelectric actuators as element of intelligent structures, *American Institute of Aeronautics and Astronautics Journal* 25 (1987) 1273–1385.

[2] M. Arockiasamy, P.S. Neelakanta, G. Sreenivasan, Vibration control of beams with embedded smart composite material, *Journal of Aerospace Engineering* 5 (4) (1992) 492–498.

[3] W.S. Hwang, H.C. Park, Finite element modeling of piezoelectric sensors and actuators, *American Institute of Aeronautics and Astronautics Journal* 30 (3) (1993) 772–780.
[4] A. Baz, S. Poh, J. Ro, J. Gilheany, Control of the natural frequencies of nitinol-reinforced composite beam, *Journal of Sound and Vibration* 185 (1) (1995) 171–185.
[5] Y.K. Kang, W. Hwang, K.S. Han, Optimum placement of piezoelectric sensor/actuator for vibration control of laminate beams, *American Institute of Aeronautics and Astronautics Journal* 34 (9) (1996) 1921–1926.
[6] J.H. Han, K.H. Rew, I. Lee, An experimental study of active vibration control of composite structures with a piezo-ceramic actuator and piezo-film sensor, *Smart Material and Structures* 6 (5) (1997) 549–558.
[7] C.P. Smyser, K. Chandrashekhara, Robust vibration control of composite beams using piezoelectric devices and neural networks, *Smart Material and Structures* 6 (2) (1997) 178–189.
[8] N.J. Hoff, *Sandwich Constructions*, Wiley, New York, 1966.
[9] F.J. Plantema, *Sandwich Construction*, Wiley, New York, 1966.
[10] H.G. Allen, *Analysis and Design of Structural Sandwich Panels*, Pergamon Press, Oxford, 1969.
[11] A.K. Noor, W.S. Burton, C.W. Bert, Computational models for sandwich panels and shells, *Applied Mechanics Review* 49 (3) (1996) 155–199.
[12] C. Hwu, J.S. Hu, Buckling and postbuckling of delaminated composite sandwich beams, *American Institute of Aeronautics and Astronautics Journal* 30 (7) (1992) 1901–1909.
[13] J.S. Hu, C. Hwu, Free vibration of delaminated composite sandwich beams, *American Institute of Aeronautics and Astronautics Journal* 33 (9) (1995) 1–8.
[14] J.S. Moh, C. Hwu, Optimization for buckling of composite sandwich plates, *American Institute of Aeronautics and Astronautics Journal* 35 (5) (1997) 863–868.
[15] R.M. Jones, *Mechanics of Composite Materials*, Scripta, Washington, DC, 1975.
[16] G.R. Cowper, The shear coefficient in timoshenko's beam theory, *Journal of Applied Mechanics* 3 (2) (1966) 335–340.
[17] L. Meirovitch, *Dynamics and Control of Structures*, Wiley, New York, 1990.
[18] W.C. Chang, Vibration Analysis and Control of Composite Sandwich Beams, M.S. Thesis, Institute of Aeronautics and Astronautics, National Cheng Kung University, Taiwan, ROC, 2000.
[19] K.M. Ahmed, Dynamic analysis of sandwich beams, *Journal of Sound and Vibration* 21 (3) (1972) 263–276.
[20] J.D. Mead, S. Sivakaumran, The stodola method applied to sandwich beams vibration, *Proceedings of the Symposium Numerical Methods for Vibration Problems*, University of Southampton, 1966.